

Print fidelity assessment for 3D food printed designs using manual and automated approaches

A K M Ahasun Habib^{1,✉}, Md Ibrahim Khalil¹, Farnaz Maleky², Ranadip Pal³
and Paul F Egan¹

¹ Department of Mechanical Engineering, Texas Tech University, USA,

² Department of Food Science and Technology, Ohio State University, USA,

³ Department of Electrical & Computer Engineering Texas Tech University, USA

✉ akhabib@ttu.edu

ABSTRACT: The ability to modify designs, personalize nutrition, and improve food sustainability makes 3D food printing (3DFP) an exciting emerging technology. Food materials' complex chemistry and mechanics make it difficult to consistently print designs of different shapes. This research uses two methods to assess printed food fidelity: Manual and automated image analysis with custom-developed algorithm. Fidelity based on printed area was measured for three overhang designs (0°, 30°, and 60°) and three food ink mixtures. The manual method provided a baseline for analysis by comparing printed images with CAD images. Both methods showed consistent results with only $\pm 3\%$ differences in analyzing printed design areas. While the computational method offers advantages for efficiency and bias reduction, making it well-suited for fidelity assessment to assess designs.

KEYWORDS: 3D printing, artificial intelligence, additive manufacturing, image analysis, automation

1. Introduction

Additive manufacturing is of significant interest for 3D food printing (3DFP) applications due to the wide range of possibilities concerning customization, personalized nutrition, and creation of novel designs (Chirico Scheele et al., 2023; Zhou et al., 2024). However, these advancements are hindered by a need to ensure that food designs are reliably fabricated and assessed for geometric fidelity (Alghamdy et al., 2024). The inherent complexities of soft food materials and design variations often result in printed objects that deviate significantly from their digital counterparts (Hussain et al., 2022). Addressing this challenge is vital for the broader adoption of food printing by consumers and practical application of 3DFP technology in food design innovation (Chirico Scheele et al., 2022). 3DFP offers flexible design creation for many applications in food including medical need and culinary creativity (Dankar et al., 2018; Zhang et al., 2022). Additionally, 3DFP is poised to aid in medical applications for eating disorders, swallowing difficulties, and providing consistent food delivery in clean environments to reduce allergens (Sundarsingh et al., 2024). Here, we consider the creation of an automated tool to efficiently assess the fidelity of printed food designs. The automated method directly supports quicker assessment in food ink formulations and geometric fidelity, leading to consistent 3D food printing assessments when directly compared to manual measurements that are potentially labor-intensive and subjective. These advancements may benefit a range of applications, including personalized nutrition, specialized medical diets, and culinary innovation, ultimately facilitating broader commercial and clinical adoption of 3D food printing technology.

3DFP is a process that applies a layer-by-layer manufacturing technique based on a predesigned digital model created through a computational aided-design (CAD) software (Tan et al., 2018). Multiple different methods exist for 3D printing food: Extrusion-based, selective sintering, inkjet, and binder jetting (Jiang et al., 2022). These processes enable printing of a wide variety of food ingredients. One of

these technologies that has recently gained visibility in the food business is extrusion-based printing (Lazou, 2024). A three-dimensional design is created by first layer-by-layer deposition using food inks that are extruded via a nozzle. Screws, pistons, or pneumatic systems (compressed air) provide the necessary force to extrude the material (Wang et al., 2023). Even though extrusion printing is becoming more popular for use in the food industry, there are new challenges to overcome in terms of making sure that soft food components retain their form once printed (Hussain et al., 2022; Sharma et al., 2024). One of the common defects in extrusion-based 3D food printing is under- or over-extrusion of filaments due to improper extrudability and the creation of a “die swell” (i.e. expanded extruded filament width) by food materials which drives a need for quality control on assessing print fidelity.

Assessing fabrication accuracy and shape fidelity rely on comparing the printed product’s dimensions with the original CAD design. Unfortunately, structural instability in many 3D-printed foods results in shapes that do not accurately reflect their digital designs (Alghamdy et al., 2024; Kadival et al., 2023). Shapes printed from different food ink mixtures reach different levels of accuracy and fidelity based on their physical properties, for instance too high of water content can lead to unstable structures while adding ingredients that increase firmness, such as proteins, can lead to higher structural stability (Chirico Scheele et al., 2023).

Typically, research in food printability has relied on manual measurements of structural dimensions to assess printability (Huang et al., 2020; Lu et al., 2023; Wen et al., 2024). While 3D scanning is used in 3D printing for geometric comparisons, it presents several challenges when applied to 3DFP. The soft and deformable nature of food materials makes it difficult to capture an accurate scan, while surface reflectivity issues, high equipment costs, and complex data processing also make 3D scanning less practical for rapid assessments in food printing (Derossi et al., 2021; Nachal et al., 2019). In comparison, a 2D image-based analysis approach has greater computational efficiency and ease of use making it highly suitable for initially evaluating geometric fidelity in 3DFP. These measurements provide an assessment of how well different shapes print but are time consuming to conduct and can also introduce subjectivity from how different people may measure an object, thus suggesting automated assessment with image analysis could address this problem more efficiently (Mustać et al., 2023). Several machine vision methods have been developed to keep up with the digitalization and smart processing revolution in the food production industry (Ding et al., 2023), thus demonstrating the importance of automation for food quality assessment. Thus, in the case of 3D food printing, automated image analysis shows promise for improving printing efficiency and quantifying printing mistakes. To better understand and quantify these challenges, this study proposes a systematic workflow for evaluating the geometric fidelity of printed food structures, as depicted in Figure 1.

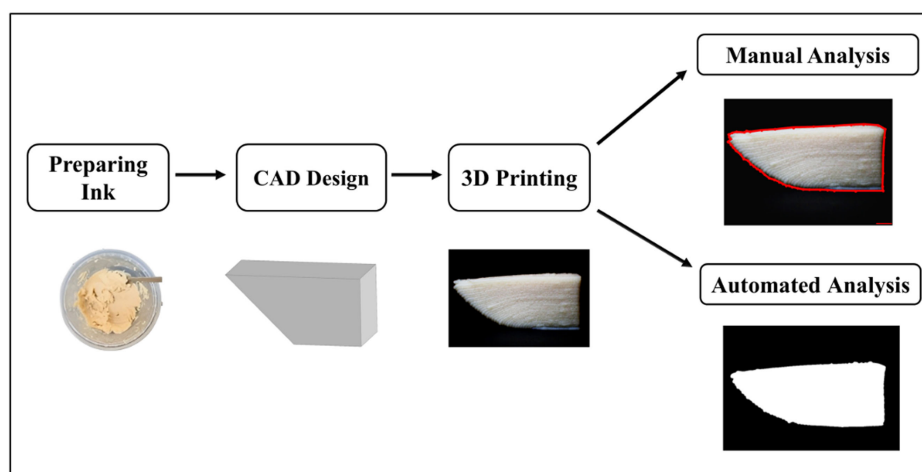


Figure 1. Workflow for 3D printing fidelity assessment with manual or automated analysis

Figure 1 outlines the step-by-step approach undertaken in this research. It begins with the preparation of food inks that include a starch-based potato ink and a protein-based pea ink, followed by the design of 3D shapes using CAD software, then printing, and finally fidelity analysis. The printing process involves the layer-by-layer deposition of food materials to create physical samples, which are then captured as images. Image processing techniques, such as grayscale conversion and binary thresholding,

are used to compare the CAD model to the printed object. The fidelity of the printed samples is assessed through both manual and automated computational methods, enabling the identification of geometric deviations and structural inconsistencies. The study systematically varies the overhang angles of printed designs from no overhang to a 60-degree overhang. By analyzing varying overhang geometries and material compositions, this study highlights the strengths and limitations of different inks to create structurally stable objects and the accuracy of both manual and automated analysis methods.

For this work the following two research questions are investigated: Q1. How accurately can 3D food printers reproduce complex geometries, such as overhang designs, compared to their original CAD models under varying design complexities for different ink materials? Q2. How well does automated computational analysis perform compared to manual processing in assessing geometric fidelity and how can automation make 3D food printing assessments faster and repeatable? Answering these questions will provide significant advances in design for assessment of 3D printed foods that will result in generalizable approaches applicable to further 3D printing technologies. The paper proceeds as follows: Section 2 describes the food ink materials, 3D printing process, and methods for fidelity evaluation. Section 3 presents and discusses results from manual and automated methods. Section 4 highlights key findings, and implications when comparing both methods, while Section 5 concludes with contributions and future research directions. For designers, the findings provide actionable insights into optimizing material formulations and design parameters, enabling more accurate and reliable fabrication of intricate structures for food printing.

2. Materials and methodology

2.1. Design generation

Three-dimensional (3D) design models were developed using CAD software (SolidWorks 2024). The initial objective of the design process was to portray the impact of varying overhang angles on structural stability by developing three models with 0°, 30°, and 60° overhang dimensions. Based on other 3D printing processes, the maximum feature size of overhangs is approximately 45 degrees for standard fused deposition modeling (Alabd & Temiz, 2024; Eryıldız, 2021). These designs were selected to evaluate the capability of 3D food printing systems to reproduce structures with angular features while maintaining geometric fidelity by changing moisture and ink composition. CAD models were exported as STL (Standard Tessellation Language) files, which were subsequently imported into the printing platform for layer-by-layer manufacturing.

2.2. Ink preparation and printing

For the preparation of food inks, mashed potato flakes (Great Value), pea protein powder (Now SPORTS), and bottled water (kirkland) were used. The pea protein powder contains 3% carbohydrates and 73% protein, while the potato flakes consist of 82% carbohydrates and 9% protein. The percentages provided account only for carbohydrates and protein, as these were the key components analyzed in this study. The mashed potato mixture was prepared by combining mashed potato flakes with water in a 1:6 ratio. The pea protein mixture was prepared by mixing pea protein powder with water in a 1:3 ratio. In a recent study, minor adjustments were made to the component mixture ratios and moisture content to evaluate their impact on printability (Khalil et al., 2024). For this study, we followed the same mixture and ratios. The weight of each component in a 100-gram mixture is presented in Table 1.

Table 1. Mass of components in 100 g food ink mixture

Mixture Type	Water	Mashed Potato	Pea Protein
Mashed Potato (MP)	85.7	14.3	0.0
Mashed Potato w/Pea Protein (MP+PP)	80.4	7.1	12.5
Pea Protein (PP)	75.0	0.0	25.0

The mashed potato combination served as the control food ink against food inks enriched with pea protein. For improving nutrition and printability, two experimental samples were prepared: one with a pea protein combination (PP) and another with a 50% mashed potato and 50% pea protein mixture (MP+PP). The mashed potato (MP) combination was first made by mixing the pre-packaged mashed potatoes with water. At the same time, a combination of pea protein (PP) and water was made. Afterwards, a mashed potato and pea protein blend (MP+PP) was made by combining the two combinations in equal weights, with each mixture accounting for one third of the total weight. The water was preheated to 65°C to facilitate consistent mixing of the ingredients. To ensure the mixture was at a consistent temperature before putting it into a syringe for printing, it was given 20 minutes to cool down to room temperature (25°C). The proposed combinations, depicted in Table 1 were printed using a Procusini 3.0 Double System (Procusini, Germany) as shown in Figure 2.

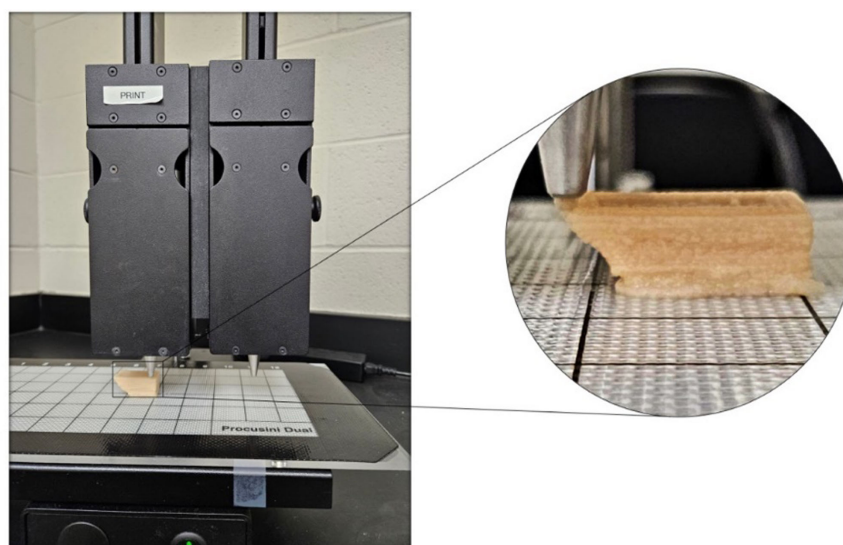


Figure 2. Procusini 3.0 dual-system food printer exhibiting food printing

The printing setup uses a layer-by-layer build-up technology, allowing precise control over food structure formation (Tan et al., 2018). The printer is equipped with two 60 mL stainless steel cartridges, specifically designed to work with a variety of edible materials, ensuring optimal performance in handling temperature-sensitive ingredients. It allows users to import CAD files from conventional CAD programs. During the printing process, a nozzle with a diameter of 1.2 mm was used and the printing speed was 10 mm/s. The nozzle movement speed varied between 5 mm/s and 200 mm/s. Throughout the printing process, the extrusion temperature remained at 25°C. The infill density was set at 50% and each layer has a height of 0.55 mm.

2.3. Print fidelity assessment

2.3.1. Image acquisition and preprocessing

Once printed, images were captured for sampling purposes. A digital camera (Olympus Tough TG-6 4 K) was used to take photos of the printed samples. The camera was placed steady on a tripod and angled at a fixed position throughout the imaging to guarantee that the photographs were taken consistently with a black background. Within 10 minutes of the printing process being completed, all the photos were captured for each print. The setup ensured controlled lighting and a fixed camera-to-sample distance to maintain image consistency. Calibration steps included white balancing and scale reference integration for accurate measurements.

2.3.2. Manual measurement

ImageJ (Software version 1.54g) was used to measure and compare the areas of a CAD model and a corresponding printed object. The manual measurements of printed parts, obtained using calipers for ground truth validation, have been previously reported in Khalil et al. (2024) that provide a reference for dimensional accuracy in 3D food printing and complement the fidelity analysis presented in this study. The analysis began with resizing both images to the same pixel dimensions to standardize the scale across the datasets, ensuring accurate area comparisons. The CAD image, which had known real-world dimensions, was used as the reference for scale calibration. Using a global scaling approach, pixel-based measurements were converted into meaningful physical units, ensuring standardized comparisons across all datasets. This process provided a consistent framework for evaluating dimensional discrepancies between CAD models and printed objects. CAD model dimensions are known and used to set the global measurement scale. This global scale was then applied consistently to all subsequent measurements for the print images. The scaling step was used only to establish a consistent unit scale across CAD and printed images, without altering or normalizing shape discrepancies inherent in the printed parts. To mitigate the risk of losing discrepancies due to scaling, it was ensured that preservation of the original aspect ratios remains unchanged during image preprocessing. The boundaries of the regions of interest in both the CAD and printed item pictures were created by the user utilizing a manual boundary selection approach using polygons. Once polygons are drawn and enclosed, the measurement provides areas for both CAD and printed images. The degree to which the printed item conforms to its CAD design may be determined by comparing these two region areas, the percentage of area error (P) is a direct reflection of the print fidelity that was calculated using below equation:

$$P = \left(\frac{A_{CAD} - A_{PRINT}}{A_{CAD}} \right) * 100 \quad (1)$$

where A_{CAD} is the area of the original CAD model and A_{PRINT} is area of printed part. The method provides a basis for evaluating dimensional discrepancies and assessing the accuracy of the printing process by manual measurement techniques.

2.3.3. Automated computational analysis

This automated analysis follows a systematic approach consisting of three key steps: Preprocessing, feature extraction, and contour area analyses. This approach was implemented using Python with OpenCV and NumPy libraries, which enabled efficient and consistent evaluation of the geometric fidelity of printed samples.

The first preprocessing step in the automated pipeline involved preparing the images for analysis. The captured images were converted to grayscale, reducing the computational complexity by eliminating color information while preserving the intensity details necessary for contour detection. Next, Gaussian blurring was applied to minimize high-frequency noise, which can interfere with edge detection. This process retained the key structural features of the object. Subsequently, during the smoothing process, binary thresholding was applied using Otsu's method. Otsu's algorithm automatically computes an optimal threshold, which divides the image into foreground (object) and background (non-object) regions based on pixel intensity distributions. This thresholding resulted in a clean binary image where the object was represented in white (pixel value 255) and the background in black (pixel value 0), providing clear segmentation of the object's shape. Additionally, to ensure that the images of the CAD model and the printed object could be compared accurately, dynamic resizing and padding were employed. Both images were resized to a common target size while preserving their aspect ratios. When necessary, padding was added to the images to ensure consistent dimensions between the two, avoiding any distortion that might arise from direct resizing. This process guaranteed that the structural details of the images remained intact while allowing for a fair comparison.

Once the preprocessing steps were complete, the next stage involved identifying and extracting the contours of the objects. Contours, which represent the boundaries of objects in an image, were detected using OpenCV's 'find Contours' function. The algorithm traced the outermost boundaries of the objects from the binary image. From the detected contours, the largest contour was selected, as it corresponded to the primary structure of interest—the main geometric shape of the object. Although the largest contour was selected, multiple contours were occasionally detected due to minor internal inconsistencies such as air bubbles, slight surface irregularities, and subtle noise in images. By specifically isolating and analyzing the largest contour which represents the outermost

boundary—these inconsistencies are minimized, ensuring accurate measurement of the primary shape’s geometric fidelity. These points are used to describe the contour’s boundary and provide the necessary data for the next phase of analysis. By focusing on the largest contour, the algorithm isolated the most significant geometric feature of the object, ensuring that extraneous details (such as noise or internal features) did not interfere with the analysis. Forms like stars, convex or basic concave forms, polygons, and circles with well-defined, closed contours may be utilized with this process, provided discernible outlines in the binary image.

With the contours extracted, the next step was to quantify the geometric properties of the objects by calculating the area enclosed by the largest contour. The area for both the CAD model and the printed object was computed using OpenCV’s contour Area function, which provides an area measure of the region enclosed by the contour. The difference between the CAD and print image measurements serves as the primary metric for comparing the geometric fidelity of the printed objects. By integrating preprocessing, contour extraction, and area calculations into an automated pipeline, this automated analysis method successfully quantified the geometric fidelity between a CAD model and its printed counterpart.

3. Results and discussion

3.1. Manual analysis of print fidelity

The manual analysis in accessing geometric fidelity was highlighted by the error percentages across three overhang angles (0° , 30° , 60°) for three mixtures: Mashed potato (MP), mashed potato with pea protein (MP+PP), and pea protein (PP). Figure 3 showcases the images with manually drawn polygon used for area calculations highlighted in yellow. The images illustrate the influence of overhang angle on the fidelity of the printed samples. At lower angles (0° and 30°), the printed structures were more consistent with their CAD models, exhibiting minimal deformation. However, at 60° , significant deviations were observed, particularly in MP samples, which showed noticeable distortions and reduced geometric accuracy. These findings also highlight the limitations of materials with lower protein content in maintaining fidelity under complex geometric conditions.





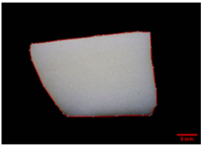







Slope of Overhang ($^\circ$)			
	0°	30°	60°
CAD Design			
MP			
MP+PP			
PP			

Figure 3. Printed images with areas traced using manual analysis (Scalebar: 5mm)

Area error percentage for each sample was calculated by Equation 1. Data was organized by material types (MP, MP+PP, PP) and overhang angles (0° , 30° , and 60°), enabling a structured comparison of geometric fidelity for different experimental conditions shown in Table 2.

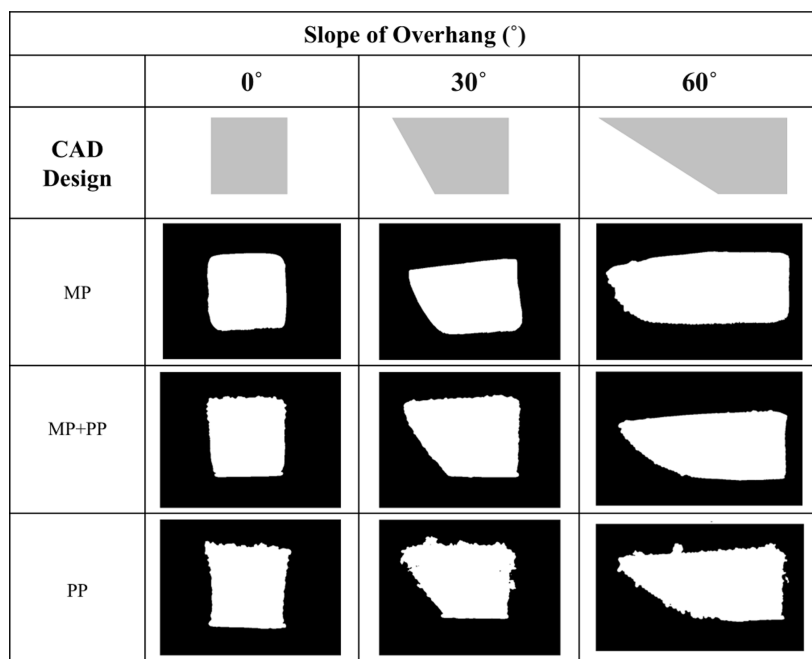
Table 2. Manual print area percentage error (%) compared to CAD models

Food Ink Mixture	Manual Measurement Area Error (%)		
	0°	30°	60°
MP	3.58%	3.92%	7.93%
PP+MP	4.04%	3.35%	4.93%
PP	7.38%	3.87%	2.82%

As shown in Table 2, the error percentages change as overhang angles changes and as the ink mixture varies. For example, the MP mixture performs poorly at 60° due to its high moisture content, which weakens its structural integrity and causes significant sagging and deformation under the stress of the steep overhang angle. PP has second highest error (7.38%) at 0° because high protein content in the ink is prone to forming uneven or rough extruded filaments. This irregular flow results in surface inconsistencies as the material may not spread or settle evenly. At 30° and 60° the higher protein content enhances its structural stability, allowing it to better maintain shape at steeper angles. Due to its well-balanced composition, MP+PP mixture has consistent error across all angles. It combines the structural rigidity of pea protein with the smooth extrusion qualities of mashed potato in reducing distortion under greater angles, to ensure consistent layer deposition. There also appears to be a systematic bias in data towards measuring structures as smaller than expected from the CAD which could be due to non-optimized printing parameters.

3.2. Automated analysis of print fidelity

By employing a custom Python-based pipeline (discussed in Section 2.3.3) for CAD and printed images. Thresholded images across all mixtures are shown in Figure 4 that isolate the structures from their backgrounds and enabling contour detection. This automated approach ensured consistent and accurate fidelity measurements while minimal user interactions.

**Figure 4. Thresholded binary images for contour area calculations**

The thresholded images across various mixtures and angles are crucial in this analysis, as it ensures clarity of structural boundaries, enabling accurate computation of the object's area. Later, it provides a quantitative comparison (Table 3) of how closely the printed structures match their corresponding CAD models.

Table 3. Automated print area percentage error (%) compared to CAD models

Food Ink Mixture	Automated Measurement Area Error (%)		
	0°	30°	60°
MP	2.09%	3.82%	10.20%
PP+MP	3.90%	2.74%	3.54%
PP	6.32%	4.59%	4.56%

The results in Table 3 align closely with the trends found in Table 2 from the manual analysis. This consistency highlights the reliability and robustness of the computational method in replicating the findings of the manual approach. Both methods demonstrate that varying geometric overhang angle and ink compositions influence print fidelity. As shown in Table 3, the error percentages in contour area calculations follow a similar trend as observed in Table 2. For instance, the MP records the highest error at 60° (10.20%), while the PP mixture has the second-highest error at 0° (6.32%) in area differences. The MP+PP mixture maintains the most consistent errors across all angles, reflecting its balanced composition, which combines the firmness of pea protein and the smooth flow properties of mashed potato. This balance ensures uniform layer deposition and minimizes deformation for challenging overhang geometries.

3.3. Comparison of manual and automated analysis

Table 4 was created by finding the difference in the Area error (%) values presented in Tables 2 and 3, which report the results of manual and automated methods, respectively. Specifically, the difference between the error percentages of the manual and automated methods was calculated to quantify the discrepancy between the two methods, allowing for a direct comparison of their performance across varying levels of overhang angles and material compositions. The resulting values, as shown in Table 4, provide insights into the degree of consistency between manual and automated assessments of 3D printing fidelity. The closer the value to zero, the more similar both methods were, indicating high agreement in fidelity assessment across all overhang designs and ink mixtures. This consistency reinforces the reliability of the automated approach in replicating manual measurements.

Table 4. Error trends across manual and automated approaches

Food Ink Mixture	Manual vs. Automated: Difference in Error Assessments		
	0°	30°	60°
MP	1.49%	0.10%	-2.27%
PP+MP	0.14%	0.61%	1.39%
PP	1.06%	-0.72%	-1.74%

Negative and positive values in Table 4 represent the direction of the discrepancy between the manual and automated error measurements, and their relationships enable assessment of the reliability and consistency of the two methods. The computational approach closely replicated the manual results, with minor differences in error percentages. The differences remain small across all angles and materials, with values all within $\pm 3\%$, reinforcing the reliability of the computational method to replicate manual measurements. Positive values indicate that the manual method measured a slightly higher error percentage compared to the automated method. This could be attributed to user subjectivity or challenges in precisely defining boundaries during manual area calculations. A negative value implies that the automated method produced a slightly higher error percentage, potentially due to sensitivity in detecting edges or overemphasizing minor structural inconsistencies. Manual contours may overlook finer edges or structural irregularities, while the automated approach may be more sensitive to minor details as key sources of errors to consider. Overall, there was high agreement between the two methods which highlights their capacity to assess food print fidelity compared to CAD models, and for the automated method to complete the task with high efficiency.

4. Conclusion

This research investigated emerging 3DFP technology with a focus on geometric fidelity assessment. Ensuring geometric fidelity in 3D food printing is critical for designers who want to deliver reliable, customizable, and visually appealing products. From personalized nutrition to complex aesthetic designs, fidelity directly impacts the functionality and consumer appeal of printed food structures. In addressing Research Question 1, this study confirms that 3D food printers can reproduce overhang designs with varying accuracy, where selection of the food ink composition and overhang angles play a pivotal role. By optimizing the combination of material mixtures and overhang angles, overhang designs in 3D food printing can achieve higher fidelity, as demonstrated by the consistent performance of balanced mixtures such as the mashed potato with pea protein ink (MP+PP) across varying design complexities.

For Research Question 2 it is supported since there is comparable error (%) trend between the manual and automated fidelity assessment methods. The automated approach can prove to be as effective as manual measurements with differences in error percentages within $\pm 3\%$. The automated approach offers enhanced consistency, scalability, and reduced human variability, making it a robust tool for assessing 3D food print fidelity. In research and industry, the automated technique decreases analysis time and labor, making it suited for analyzing larger datasets of print images or iterative design cycles. The automated approach's repeatable outcomes enhance reliability, making it a dependable alternative to manual methods.

The study primarily assesses fidelity through area calculations; however, future work could expand the scope to include additional geometric parameters such as height, surface smoothness, and structural consistency to provide a more comprehensive evaluation. Furthermore, this method can be extended to more complex 3D geometries by integrating multi-view imaging and AI-driven 3D reconstruction techniques, which will enhance accuracy and applicability for intricate food structures. Overall, the current work establishes a systematic and scalable means of determining print fidelity, automating the assessment process, and laying the foundation for future innovations in food ink formulations and geometric design within the evolving field of food printing.

Acknowledgements

“Funding for this research was supported by the United States Department of Agriculture (USDA) Grant 2023-67017-40745 “Characterization of 3D printed protein inks with customization using machine learning.”

References

- Alabd, M. U., & Temiz, A. (2024). Optimization of annealing and 3d printing process parameters of pla parts. *International Journal of 3D Printing Technologies and Digital Industry*, 8(2), 185–201. <https://doi.org/10.46519/ij3dptdi.1451666>

- Alghamdy, M., He, I., Satsangee, G.R., Keramati, H., & Ahmad, R. (2024). Enhancing Printability Through Design Feature Analysis for 3D Food Printing Process Optimization. *Applied Sciences*, 14(20), 9587. <https://www.mdpi.com/2076-3417/14/20/9587>
- Chirico Scheele, S., Binks, M., Christopher, G., Maleky, F., & Egan, P.F. (2023). Printability, texture, and sensory trade-offs for 3D printed potato with added proteins and lipids. *Journal of Food Engineering*, 351, 111517. <https://doi.org/10.1016/j.jfoodeng.2023.111517>
- ChiricoScheele, S., Hartmann, C., Siegrist, M., Binks, M., & Egan, P.F. (2022). Consumer Assessment of 3D-Printed Food Shape, Taste, and Fidelity Using Chocolate and Marzipan Materials. *3D Print Addit Manuf*, 9(6), 473–482. <https://doi.org/10.1089/3dp.2020.0271>
- Dankar, I., Haddarah, A., Omar, F.E.L., Sepulcre, F., & Pujolà, M. (2018). 3D printing technology: The new era for food customization and elaboration. *Trends in Food Science & Technology*, 75, 231–242. <https://doi.org/10.1016/j.tifs.2018.03.018>
- Derossi, A., Caporizzi, R., Paolillo, M., & Severini, C. (2021). Programmable texture properties of cereal-based snack mediated by 3D printing technology. *Journal of Food Engineering*, 289, 110160. <https://doi.org/10.1016/j.jfoodeng.2020.110160>
- Ding, H., Tian, J., Yu, W., Wilson, D.I., Young, B.R., Cui, X., Xin, X., Wang, Z., & Li, W. (2023). The application of artificial intelligence and big data in the food industry. *Foods*, 12(24), 4511.
- Eryıldız, M. (2021). Effect of Build Orientation on Mechanical Behaviour and Build Time of FDM 3D-Printed PLA Parts: An Experimental Investigation. *European Mechanical Science*, 5(3), 116–120. <https://doi.org/10.26701/ems.881254>
- Huang, M.-S., Zhang, M., & Guo, C.-F. (2020). 3D printability of brown rice gel modified by some food hydrocolloids. *Journal of Food Processing and Preservation*, 44(7), e14502. <https://doi.org/10.1111/jfpp.14502>
- Hussain, S., Malakar, S., & Arora, V.K. (2022). Extrusion-Based 3D Food Printing: Technological Approaches, Material Characteristics, Printing Stability, and Post-processing. *Food Engineering Reviews*, 14(1), 100–119. <https://doi.org/10.1007/s12393-021-09293-w>
- Jiang, Q., Zhang, M., & Mujumdar, A.S. (2022). Novel evaluation technology for the demand characteristics of 3D food printing materials: A review. *Critical Reviews in Food Science and Nutrition*, 62(17), 4669–4683.
- Kadival, A., Kour, M., Meena, D., & Mitra, J. (2023). Extrusion-based 3D food printing: printability assessment and improvement techniques. *Food and Bioprocess Technology*, 16(5), 987–1008.
- Khalil, M. I., Maleky, F., Pal, R., & Egan, P.F. (2024). Manufacturability of Protein-Reinforced Foods With Overhang Designs. *ASME 2024 International Design Engineering Technical Conferences and Computers and Information in Engineering Conference*.
- Lazou, A. E. (2024). Food extrusion: An advanced process for innovation and novel product development. *Critical Reviews in Food Science and Nutrition*, 64(14), 4532–4560. <https://doi.org/10.1080/10408398.2022.2143474>
- Lu, Y., Rai, R., & Nitin, N. (2023). Image-based assessment and machine learning-enabled prediction of printability of polysaccharides-based food ink for 3D printing. *Food Research International*, 173, 113384. <https://doi.org/10.1016/j.foodres.2023.113384>
- Mustač, N. Č., Pastor, K., Kojić, J., Voučko, B., Čurić, D., Rocha, J.M., & Novotni, D. (2023). Quality assessment of 3D-printed cereal-based products. *LWT*, 115065.
- Nachal, N., Moses, J.A., Karthik, P., & Anandharamakrishnan, C. (2019). Applications of 3D Printing in Food Processing. *Food Engineering Reviews*, 11(3), 123–141. <https://doi.org/10.1007/s12393-019-09199-8>
- Sharma, R., ChandraNath, P., KumarHazarika, T., Ojha, A., Kumar Nayak, P., & Sridhar, K. (2024). Recent advances in 3D printing properties of natural food gels: Application of innovative food additives. *Food*
- Sundarsingh, A., Zhang, M., Mujumdar, A.S., & Li, J. (2024). Research progress in printing formulation for 3D printing of healthy future foods. *Food and Bioprocess Technology*, 17(11), 3408–3439.
- Tan, C., Toh, W.Y., Wong, G., & Li, L. (2018). Extrusion-based 3D food printing - Materials and machines. *Int J Bioprint*, 4(2), 143. <https://doi.org/10.18063/IJB.v4i2.143>
- Wang, C., Yan, R., Li, X., Sang, S., McClements, D.J., Chen, L., Long, J., Jiao, A., Wang, J., & Qiu, C. (2023). Development of emulsion-based edible inks for 3D printing applications: Pickering emulsion gels. *Food Hydrocolloids*, 138, 108482.
- Wen, Y., Che, Q.T., Wang, S., Park, H.J., & Kim, H.W. (2024). Elaboration of dimensional quality in 3D-printed food: Key factors in process steps. *Comprehensive Reviews in Food Science and Food Safety*, 23(1), e13267.
- Zhang, J. Y., Pandya, J.K., McClements, D.J., Lu, J., & Kinchla, A.J. (2022). Advancements in 3D food printing: a comprehensive overview of properties and opportunities. *Critical Reviews in Food Science and Nutrition*, 62(17), 4752–4768. <https://doi.org/10.1080/10408398.2021.1878103>
- Zhou, L., Miller, J., Vezza, J., Mayster, M., Raffay, M., Justice, Q., Al Tamimi, Z., Hansotte, G., Sunkara, L.D., & Bernat, J. (2024). Additive Manufacturing: A Comprehensive Review. *Sensors*, 24(9), 2668. <https://www.mdpi.com/1424-8220/24/9/2668>